

# Ultrathin corundum-type $\text{In}_2\text{O}_3$ nanotubes derived from orthorhombic $\text{InOOH}$ : synthesis and formation mechanism†

Changlong Chen, Dairong Chen,\* Xiuling Jiao\* and Cuiqing Wang

Received (in Cambridge, UK) 14th July 2006, Accepted 14th September 2006

First published as an Advance Article on the web 28th September 2006

DOI: 10.1039/b610120h

Single-crystalline metastable corundum-type  $\text{In}_2\text{O}_3$  nanotubes were prepared by annealing solvothermally synthesized  $\text{InOOH}$  nanotubes under ambient pressure at 300 °C, and the formation mechanism of the nanotubes was investigated.

As n-type semiconducting oxide of the III–VI compounds, indium oxide ( $\text{In}_2\text{O}_3$ ) nanostructures possess novel electronic and optical properties resulting from quantum size confinement of carriers and hold great promise for applications in areas including nanoelectronics, electro-optics, photocatalysis and photoelectrochemistry.  $\text{In}_2\text{O}_3$  usually exhibits a stable cubic bixbyite-type structure.<sup>1</sup> In the past few years, to meet different requirements, many efforts have been made to prepare cubic  $\text{In}_2\text{O}_3$  nanostructures with different morphologies such as nanoparticles (nanocrystals or quantum dots),<sup>2</sup> nanowires,<sup>3</sup> nanobelts,<sup>4</sup> nanocrystal chains,<sup>5</sup> pyramid-like crystals,<sup>6</sup> nanotubes filled with metal indium,<sup>7</sup> etc.<sup>8</sup> Recently, the metastable corundum-type (hexagonal structure)  $\text{In}_2\text{O}_3$ , a high-pressure modification, has become particularly attractive because the metastable phase is a route toward creating new materials,<sup>9</sup> but few studies on the preparation and properties of corundum-type  $\text{In}_2\text{O}_3$ , especially its nanostructures, have been reported. By annealing the  $\text{InOOH}$  precursor at ambient pressure, Gurlo *et al.* synthesized corundum-type  $\text{In}_2\text{O}_3$  particles,<sup>10</sup> and Qian's group prepared corundum-type  $\text{In}_2\text{O}_3$  nanofibers.<sup>11</sup> However, to the best of our knowledge, the synthesis of corundum-type  $\text{In}_2\text{O}_3$  tubular structures, especially single-crystalline  $\text{In}_2\text{O}_3$  nanotubes with narrow diameter and uniform geometry, has not been reported. In this communication, we use a solvothermal route to prepare orthorhombic  $\text{InOOH}$  nanotubes, then anneal them under ambient pressure to produce corundum-type (hexagonal)  $\text{In}_2\text{O}_3$  nanotubes with closed ends.

To prepare the  $\text{InOOH}$  nanotubes,  $\text{InCl}_3 \cdot 4\text{H}_2\text{O}$  was added into anhydrous ethanol. Formamide and sodium dodecylbenzenesulfonate (SDBS) were used as the additives. After the solution was heated at 140 °C for 8 h, the precipitate was separated by centrifugation, and washed with deionized water. The X-ray diffraction (XRD) pattern shows that the product exhibits an orthorhombic  $\text{InOOH}$  structure (Fig. 1a) (JCPDS No. 71-2283). The Fourier transform infrared (FT-IR) spectrum indicates that SDBS molecules as well as hydroxyls and adsorbed water are contained in the product. Thermogravimetric analysis (TGA) demonstrates that the content of SDBS together with the adsorbed

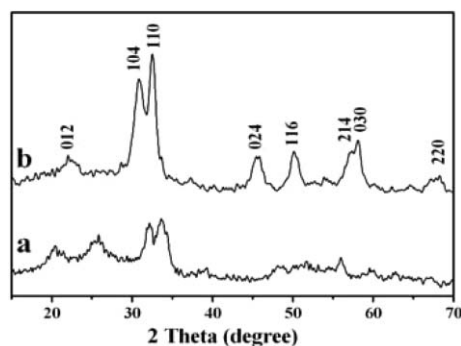


Fig. 1 XRD patterns of the precursors (a) before and (b) after annealing at 300 °C under ambient pressure.

water is *ca.* 24.4% (see ESI Fig. S1†). Transmission electron microscopy (TEM) reveals the tubular structure is end-closed, with *od ca.* 7 nm, *id* 3 nm and lengths in the range of 30–60 nm (Fig. 2a). The corresponding high resolution TEM (HR-TEM) image (Fig. 2b) shows that the nanotubes exhibit well-defined lattice fringes, indicating their single crystalline nature. The marked two groups of crystal planes are (011) and (101) planes of orthorhombic  $\text{InOOH}$ , which have the same interplanar spacing of 0.278 nm and an included angle of *ca.* 63°. It indicates that the exhibited facet is the (010) plane.

Time-dependent experiments were conducted to investigate the formation process of the nanotubes. The TEM image showed that when the reactants were heated for 0.5 h, the products were willow-leaf-like lamellas with a length of *ca.* 500 nm and width of 180 nm (Fig. 3a), which were not stable under the irradiation of the electron beam during the TEM observation. They gradually contracted into small balls and disappeared within one minute.

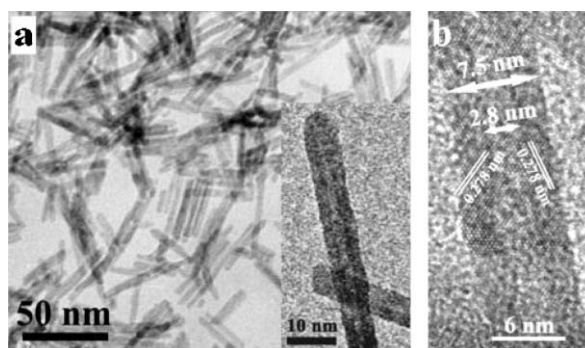


Fig. 2 (a) TEM image of  $\text{InOOH}$  nanotubes. The inset is its high-magnification TEM image. (b) HRTEM image of  $\text{InOOH}$  nanotube.

Department of Chemistry, Shandong University, Jinan, 250100, People's Republic of China. E-mail: cdr@sdu.edu.cn; Fax: +86-531-88364281; Tel: +86-531-88364280

† Electronic supplementary information (ESI) available: Experimental details, FTIR spectra, TG curves, *I-V* curves and schematic structure of FETs. See DOI: 10.1039/b610120h

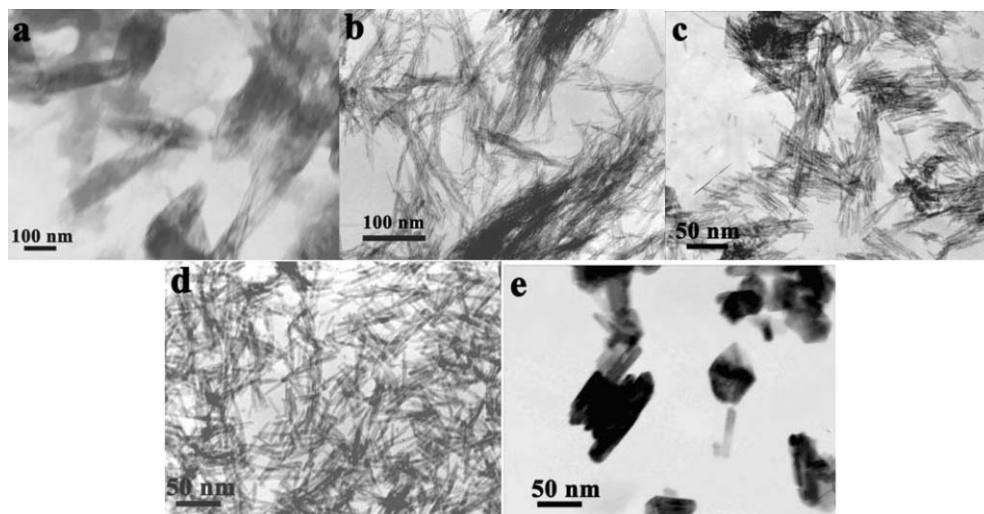


Fig. 3 TEM images of the products obtained at 140 °C with a heating time of (a) 0.5 h, (b) 2 h, (c) 5 h, (d) 9 h, and (e) 40 h.

Prolonging the reaction time to 2 h, threads with a diameter of *ca.* 2 nm (Fig. 3b) were obtained, which were stable when exposed to the electron beam. Further prolonging the reaction time caused these threads to become discrete and their diameters gradually increased. For instance, the size of the particles obtained after heating times of 5 and 9 h increased to *ca.* 4 nm and *ca.* 8 nm, respectively (Fig. 3c and d). In particular, the product after a heating time of 40 h was composed of short and thick tubes together with large irregular particles (Fig. 3e). The evolution of the product was also tracked using XRD. As shown in Fig. 4a, the product formed in the initial 0.5 h was amorphous. Upon increasing the reaction time, the products exhibit a narrow diffraction peak at  $2\theta = 22.3^\circ$  and a weak one at  $2\theta = 45.4^\circ$ , which could be indexed to the diffraction of the (200) and (400) lattice planes of cubic  $\text{In}(\text{OH})_3$  (JCPDS No. 85-1338), respectively (Fig. 4b–d). From the XRD patterns, it is found that the content of  $\text{In}(\text{OH})_3$  first gradually increased and then decreased within 4 h. When the reaction time was longer than 4 h, the diffraction peaks of the (200) and (400) lattice planes disappeared. At the same time,

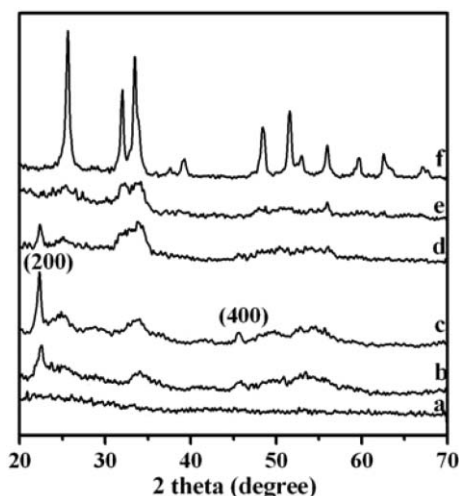
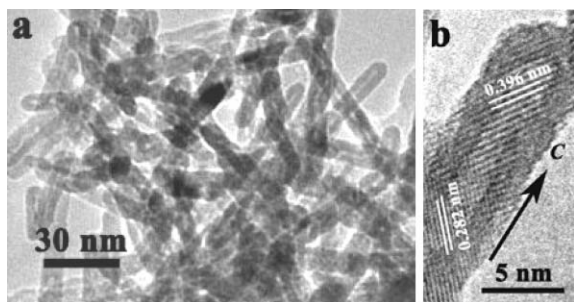


Fig. 4 XRD patterns of the products obtained at 140 °C with a heating time of (a) 0.5 h, (b) 1 h, (c) 2 h, (d) 3 h, (e) 9 h, and (f) 40 h.

some plasmon bands are also observed on all the XRD patterns (excluding the amorphous one) and they progressively become stronger with heating time (Fig. 4b–e), indicating that the product is the InOOH phase (JCPDS No. 71-2283). In particular, when the reaction time reached 40 h a highly-crystalline InOOH phase was obtained (Fig. 4f).

Based on the above information, a template-synthesis mechanism for the inorganic nanotubes is proposed. First, ion exchange occurs, in which part of the counterions of SDBS are replaced by  $\text{In}^{3+}$  ions. The complex dissolves slightly in ethanol and then self-assembles to form the lamella-like particles. Upon extended heating, the lamella particles hydrolysed to form  $\text{In}(\text{OH})_3$  nanorods, stabilized by dodecylbenzenesulfonate. As shown in Fig. 4, however, the  $\text{In}(\text{OH})_3$  dehydrolysed to form InOOH as soon as the  $\text{In}(\text{OH})_3$  formed. Over time as reactants are consumed, the dehydrolysis progressively become dominant and the hydrolysis gradually weakens. As a result, the InOOH gradually increases corresponding to the decrease of the  $\text{In}(\text{OH})_3$ . Finally, all of the  $\text{In}(\text{OH})_3$  is transformed to InOOH through dehydrolysis. Under the present solvothermal conditions, such transformation from  $\text{In}(\text{OH})_3$  to InOOH presumably occurred by ‘dissolution and recrystallization’. In this process, the preformed  $\text{In}(\text{OH})_3$  slowly dissolves due to its larger solubility compared with that of the InOOH, and then the heterogeneous nucleation and growth of new InOOH occurs on the surface of the  $\text{In}(\text{OH})_3$  nanorods. When all the  $\text{In}(\text{OH})_3$  in the inner part has dissolved, InOOH nanorods with larger diameter and hollow tubular structure are formed. Thus, the formation of InOOH nanotubes appears to use the preformed  $\text{In}(\text{OH})_3$  nanorods as templates. If the reaction time is allowed to proceed continuously, Ostwald ripening leads to the thickening of the nanotubes.<sup>12</sup> After 40 h, thick tubes together with irregular particles were obtained (Fig. 3e).

After annealing the InOOH nanotubes at 300 °C for 0.5 h under ambient pressure, a metastable corundum-type  $\text{In}_2\text{O}_3$  (JCPDS No. 22-0336) is obtained (Fig. 1b). As a high-pressure modification, the corundum-type phase usually exists at high temperature or under high pressure. The formation of the metastable corundum-type  $\text{In}_2\text{O}_3$  under mild conditions should be attributed to stabilization by the SDBS molecules on the InOOH nanotubes. The SDBS



**Fig. 5** (a) TEM image of  $\text{In}_2\text{O}_3$  nanotubes and (b) HRTEM image of one  $\text{In}_2\text{O}_3$  nanotube.

presumably decreases the surface energy and prevents phase transformation during the annealing process. The high magnification TEM image (Fig. 5a) shows that the annealed particles (same sample shown in Fig. 2) still keep the tubular structure. The HRTEM image (Fig. 5b) of a typical annealed nanotube demonstrates its continuous lattice fringes and contrast difference between the wall and hollow lumen, confirming its single crystalline and tubular structure. The  $\text{In}_2\text{O}_3$  nanotubes, exhibiting an outer diameter of ca. 5 nm and an inner diameter of ca. 2 nm, are slightly thinner than the  $\text{InOOH}$  nanotubes because of shrinkage during the dehydrolysis process. The shown fringe distances of 0.396 nm and 0.282 nm correspond to the lattice distances of the (012) and (01  $\bar{4}$ ) planes of hexagonal  $\text{In}_2\text{O}_3$ , which indicates that the nanotube is stretched along the *c* axis. The FTIR spectrum reveals that the  $\text{In}_2\text{O}_3$  nanotubes still contain the adsorbed surfactant molecules as well as water, ca. 18% from the TGA curve (see ESI Fig. S2†). Moreover, comparing the FTIR spectrum of the  $\text{In}_2\text{O}_3$  nanotubes with that of the  $\text{InOOH}$  nanotubes (ESI Fig. S1a), the peaks at  $1957\text{ cm}^{-1}$  and  $2720\text{ cm}^{-1}$ , typical of the O–H vibration of  $\text{InOOH}$ , nearly disappear. Together with the corresponding XRD patterns (Fig. 1), it is deduced that the transformation of  $\text{InOOH}$  to  $\text{In}_2\text{O}_3$  is nearly complete.

In summary, the single-crystalline metastable corundum-type  $\text{In}_2\text{O}_3$  nanotubes could be prepared by annealing the solvothermally synthesized  $\text{InOOH}$  nanotubes under ambient pressure at  $300\text{ }^\circ\text{C}$ . A template-synthesis mechanism was proposed for the

formation of  $\text{InOOH}$  nanotubes during the solvothermally procedure. FETs fabricated by the as-prepared  $\text{In}_2\text{O}_3$  nanotubes revealed stable p-type channel conduction behavior (see ESI Fig. S3, Fig. S4).

This work was supported by the Program for New Century Excellent Talents in University, P. R. China. The authors thank Dr Pamela Holt for editing the manuscript.

## Notes and references

- (a) A. Gurlo, N. Barsan, U. Weimar, M. Ivanovskaya, A. Taurino and P. Siciliano, *Chem. Mater.*, 2003, **15**, 4377; (b) K. R. Prasad, K. Koga and N. Miurapp, *Chem. Mater.*, 2004, **16**, 1845.
- (a) Q. Liu, W. Lu, A. Ma, J. Tang, J. Lin and J. Fang, *J. Am. Chem. Soc.*, 2005, **127**, 5276; (b) K. Soulantica, L. Erades, M. Sauvan, F. Senocq, A. Maisonnat and B. Chaudret, *Adv. Funct. Mater.*, 2003, **13**, 553; (c) Y. Zhang, H. Ago, J. Liu, M. Yumura, K. Uchida, S. Ohshima, S. Iijima, J. Zhu and X. Zhang, *J. Cryst. Growth*, 2004, **264**, 363; (d) W. S. Seo, H. H. Jo, K. Lee and J. T. Park, *Adv. Mater.*, 2003, **15**, 795.
- (a) C. Li, D. H. Zhang, S. Han, X. L. Liu, T. Tang and C. Zhou, *Adv. Mater.*, 2003, **15**, 143; (b) C. Liang, G. Meng, Y. Lei, F. Philipp and L. Zhang, *Adv. Mater.*, 2001, **13**, 1330; (c) M. Zheng, L. Zhang, G. Li, X. Zhang and X. Wang, *Appl. Phys. Lett.*, 2001, **79**, 839; (d) X. Peng, G. Meng, J. Zhang, X. Wang, Y. Wang, C. Wang and L. Zhang, *J. Mater. Chem.*, 2002, **12**, 1602; (e) L. Dai, X. L. Chen, J. K. Jian, M. He, T. Zhou and B. Q. Hu, *Appl. Phys. A*, 2002, **75**, 687; (f) X. Wu, J. Hong, Z. Han and Y. Tao, *Chem. Phys. Lett.*, 2003, **373**, 28; (g) J. Zhang, X. Qing, F. Jiang and Z. Dai, *Chem. Phys. Lett.*, 2003, **371**, 311; (h) F. Zeng, X. Zhang, J. Wang, L. Wang and L. Zhang, *Nanotechnology*, 2004, **15**, 596.
- (a) Z. Pan, Z. Dai and Z. Wang, *Science*, 2001, **291**, 1947; (b) X. Kong and Z. Wang, *Solid State Commun.*, 2003, **128**, 1.
- J. Lao, J. Huang, D. Wang and Z. Ren, *Adv. Mater.*, 2004, **16**, 65.
- (a) P. Guha, S. Kar and S. Chaudhuria, *Appl. Phys. Lett.*, 2004, **85**, 3851; (b) H. Jia, Y. Zhang, X. Chen, J. Shu, X. Luo, Z. Zhang and D. Yu, *Appl. Phys. Lett.*, 2003, **82**, 4146.
- Y. Li, Y. Bando and D. Golberg, *Adv. Mater.*, 2003, **15**, 581.
- B. Cheng and E. T. Samulski, *J. Mater. Chem.*, 2001, **11**, 2901.
- (a) L. Brus, *Science*, 1997, **276**, 373; (b) L. Brus, *Science*, 1997, **276**, 398.
- M. Epifani, P. Siciliano, A. Gurlo, N. Barsan and U. Weimar, *J. Am. Chem. Soc.*, 2004, **126**, 4078.
- D. Yu, S. H. Yu, S. Zhang, J. Zuo, D. Wang and Y. Qian, *Adv. Funct. Mater.*, 2003, **13**, 497.
- (a) B. L. Cushing, V. L. Kolesnichenko and C. J. O'Connor, *Chem. Rev.*, 2004, **104**, 3893; (b) H. G. Yang and H. C. Zeng, *J. Phys. Chem. B*, 2004, **108**, 3492.